Development of a Passive RFID Temperature Sensor for Wildfire Applications

A Thesis
SUBMITTED TO THE FACULTY OF THE UNIVERSITY
OF MINNESOTA
BY

Amanda M. McCann

IN PARTIAL FULFILLMENT OF THE REQUIREMENTS
FOR THE DEGREE OF
MASTER OF SCIENCE

Advisor: Dr. Lauren Linderman

May 2023

Acknowledgments

I would first like to thank my thesis advisor Dr. Linderman of the Civil Engineering department at the University of Minnesota. Dr. Linderman was always available when I had a question about my research, writing or studies. She always steered me in the right direction and helped brainstorm when I got stuck.

I would also like to thank the other experts who took part in the final review process for my thesis: Dr. Lee Frelich and Professor Boya Xiong. They both supplied good advice and pointers which helped the final writing process. Without their advice and support, the final review of my thesis could not have been successfully conducted.

I would also like to thank Mugeral Turos, a researcher at the University of Minnesota. He helped provide many of the tools and equipment used throughout my research. He also shared helpful tips and tricks to help my research move along smoothly. Without him, my research would not have gone quite as smoothly.

I would also like to thank Hugh Cunningham from Abbot Laboratories. He helped me with technical issues that arrived and with the set-up of the systems used throughout my research. Without him, this research would probably have taken much longer.

I would also like to thank the Sloan Foundation for providing me with the opportunity. Their funding and support have been appreciated throughout this process. I would also like to extend this thank you to the other researchers working under the Sloan Foundation on Wildfire research. They provided me with support throughout my graduate school journey.

Lastly, I must express my gratitude to my parents, husband and friends for providing me with continuous encouragement and support throughout my years of study and through my

process of writing my thesis. Without their support and aid, this accomplishment would not have been possible.

Abstract

Recent wildfire events in California and Oregon have resulted in localized water contamination. A potential cause is the heating of polymer-based water service lines and mains in these communities. Finding the source of contamination can be a huge burden on municipalities, taking significant resources and time. The investigation in Santa Rosa and Paradise, California took months and millions of dollars and delayed the recovery time for these communities. These contamination events highlighted the need for a quicker, more efficient way to check water lines in affected areas. Previous research has shown that the threshold temperatures that result in contamination are 194° C for polyvinyl chloride (PVC) and 250° C for high-density polyethylene (HDPE) pipes, respectively. The objective of this work is the development of a low-cost sensor system to identify potentially damaged pipelines and sources of water contamination.

The proposed solution is a radio frequency identification (RFID) based temperature sensor to indicate once a certain temperature is reached. Passive, ultra-high frequency (UHF) RFID tags are used in conjunction with a trigger mechanism that disconnects after the threshold temperature is reached over a meaningful duration. Passive RFID tags will allow for the sensor to work without the use of batteries and are low-cost. The design and characterization of the sensor utilize two experimental frameworks: (1) benchtop testing, and (2) small-scale tests in a more realistic environment. The benchtop testing identified the trigger temperature, mechanism, and reliability of the sensor design. The small-scale testing installs the sensors on buried pipes subjected to a realistic fire load. The resulting design and characterization will be presented in terms of accuracy and reliability. Additionally, the heat flux of the benchtop testing will differ from a more realistic environment, so the results will be compared to isolate how the heat flux

might impact future WUI- based sensor development. These tests will support the development of the RFID-based sensors for full-scale implementations.

Table of Contents

List of Tables

List of Figures

Chapter 1. Introduction

Recent wildfire activity has negatively impacted communities, particularly in the wild-urban interface (WUI) (Iglesias et al. 2022). Communities along the wildfire path often suffer destruction to homes, businesses, schools, and medical facilities (Schulze et al. 2020). Kramer et al. (2021) analyzed the rebuilding rates in California up to 25 years after wildfires from 1970 to 2005. The study found that 58% of the destroyed buildings were rebuilt within 3-6 years, and approximately 94% of the remaining buildings were rebuilt within 13-25 years (Kramer et al. 2021). The 2017 Tubbs fire in Santa Rosa, California destroyed 5,636 structures and damaged an additional 317 structures (Cal Fire 2019a). It is estimated that the Tubbs fire cost $9.4 billion (Cal Fire 2019a). The 2018 Camp fire in Paradise, California engulfed 18,000 acres of land in 8 hours, destroying a total of 153,000 acres of land (Cal Fire 2019b). Cal Fire (2019b) estimates that the Camp fire caused $12.5 billion in total insured losses.

Shortly after the Tubbs and Camp fires, volatile organic compounds (VOCs) such as benzene were found in the water distribution system with levels over the federal maximum containment levels (MCL) (Proctor et al, 2020; Richter et al. 2022). Typically, water distribution systems consist of water mains, meter boxes, and service laterals. Water mains are located a greater depth below the ground (depths greater than 1.07 m) than service laterals (minimum depth of 0.305 m). Approximately, 3% of the water main pipes tested in Paradise and Santa Rosa contained contaminants over the MCL (Richter et al. 2022). While 19% of service lateral pipes were found to have contaminants over the MCL (Richter et al. 2022).

Two potential causes for the contamination are the heating of the service pipeline materials or negative pressure within the system which caused backflow in the system and allowed

contaminated gases into the system (Schulze and Fisher 2021). This research is predominantly focused on the heating of pipeline materials. Prior research has found that when heated over a certain amount of time, plastic pipelines can release compounds such as benzene, toluene, ethylbenzene, xylene, chlorobenzene, and naphthalene into the air and water supply, making it dangerous to drink (Isaacson et al. 2020; Metz et al. 2022; Schulze and Fisher 2021). When subjected to this level of heat, pipelines affected by wildfires can remain structurally sound and exhibit melting or look fine at first glance. Isaacson et al. (2020) document high-density polyethylene (HDPE) pipelines affected by the wildfire burn severity.

The lack of easily accessible potable water can result in long school closures, prolonged business shutdowns, and many people being displaced from their homes (Hamideh et al. 2021). Testing the water and condition of every pipeline can be a long and expensive process, and the replacements and testing can be a main contributor to the time it takes for a community to rebuild. The contaminants caused by the Tubbs and Camp fire took more than a year to remove (Isaacson et al. 2020). Further, the 2018 Camp fire in Paradise, California caused structural damage to 6 of the 8 schools in the area, and only 2 of those schools completely collapsed due to the fire (Schulze et al. 2020). After the wildfire, schools were either combined or students were sent to neighboring schools. As of 2020, Schulze et al. (2020) found that only 4 of the schools reopened in 2019, with 2 of the schools not having available data.

Physically checking every pipeline to assess for damage or potential leaks can be costly and time-consuming, so alternative approaches have been explored. The most common form of pipe monitoring is based on fiber optic cables; these monitor an entire length of pipe and track temperature changes to detect leakage (Lin et al. 2019). The cost of a fiber optic system depends on its implementation, Badar et al. (2021) listed the cost of fiber optic temperature monitors as

$5,000 to $16,000, and the cost of fiber optic temperature sensors as $10,000. Alternatively, wireless sensing systems such as radio frequency identification (RFID) systems can be used to surveil certain points of pipelines. Vyas and Tye (2019) developed a passive RFID system that could detect leakage from pipelines, but the system requires continuous data monitoring to fully operate. To overcome challenges using buried wireless sensing, other pipeline monitoring systems use battery-powered RFID tags to propagate signals further (Lin et al. 2019).

For other temperature monitoring applications, such as monitoring electrical components, thermal exposure for vehicles, and indicators for sterilization processes, visual indicators can be implemented. Sling et al. (2009) developed a color-based time-temperature indicator, where a permanent color change occurs at specific temperatures and the color indicates the time the temperature was reached. The extension of these visual tools to pipeline monitoring could be limited given there is not often a direct line of sight to the system.

Wildfires are not constant from event to event, the ground temperatures of forest fires can range from 200° C to 800° C, depending on the location, fuel source, and atmospheric conditions (Isaacson et al. 2020). The temperature the pipelines are exposed to is also dependent on many factors, such as burial depth, thermal conductivity of the soil, the ground temperature of the fire, and proximity to other materials or fuels, which could expose the pipelines to greater temperatures. Wildfires do not have consistent intervals such that communities can fully prepare for these events either. Further, any exposed system could burn and be rendered useless during a wildfire, making it difficult to actively monitor the pipelines themselves. These factors present a challenge in the development of a pipeline monitoring system that is low maintenance, low–cost, and can withstand high temperatures to aid in the recovery of affected communities.

In this thesis, a passive ultra-high frequency (UHF) RFID temperature system is proposed for monitoring pipeline systems in WUI communities. The system uses a temperature trigger based on an internal circuit mechanism. The circuit mechanism utilizes a trigger material that is dependent on the critical temperature of the polymer pipe being monitored. Two RFID tags are utilized, one that will always be readable, and the second that will be connected to the circuit and only be operational when the threshold or critical temperature hasn't been reached. The novelty of the design lies in the passive operation of the system at high temperatures under harsh conditions. Chapters 2 and 3 provide a literature review and background on pipeline monitoring and RFID-based systems. Chapter 4 outlines the design considerations and presents the proposed sensor system. Chapter 5 reviews the performance of the proposed system in a series of benchtop and lab-scale experiments. Finally, Chapter 6 discusses conclusions and proposes future work.

Chapter 2. Literature Review: A Review of Pipeline Monitoring Systems

2.1 Pipeline Monitoring Systems

The use of wireless systems to monitor the health of pipelines can aid in the swift recovery of these water networks. Fiber optic cables can be used to monitor the health of pipelines, more specifically to detect pipeline leakage using temperature changes (Inaudi and Glisic 2010; Lin et al. 2019; Nikles 2009; Nikles et al. 2004). They can cover the entire length of the pipeline and are relatively cost-effective. In 2010, fiber optic cables allowed for 60 km of pipeline to be monitored from a single instrument. Fiber optic cables are especially helpful for the monitoring of pipes in more remote regions and areas affected by harsh environmental conditions (Nikles 2009). Some fiber optic cables can sustain a pressure of around 75 MPa and are designed to last for more than 30 years (Nikles et al. 2004). Further, they can function over a large operating temperature range based on their cables design, such -20℃ to 60℃, and -50℃ to 80℃ (Inaudi and Glisic 2010; Nikles et al. 2004). However, forest fires tend to have much larger temperature ranges and, exposing fiber optic cables to these temperatures could damage some of the temperature sensing nodes and render them useless after a forest fire.

2.2 Temperature Monitoring Systems

Temperature sensing systems are helpful for environments where exceeding a specific temperature can be detrimental, for example, perishable goods in a refrigerated environment. Permanent physical change sensors, such as color indicators, can reflect if a certain temperature was reached but not necessarily when (Crenshaw et al. 2007; Sing et al. 2009; Khan et al. 2021). The color change can be caused by specific polymers that respond to changes in heat,

deformation, chemicals, light, and many other stimuli (Crenshaw et al. 2007). Exposing these sensors to temperatures above their glass transition temperature can cause a chemical reaction that causes an irreversible change of color (Sing et al. 2009). The glass transition temperature depends on the chemicals used, generally, these can occur from 13℃ to 200 ℃ (Crenshaw et al. 2007; Sing et al. 2009).

Another sensing approach that leverages a permanent change in the system uses shape memory alloys (Caizzone et al. 2011; Khan et al. 2021). The shape memory can be used to permanently alter a sensor, which can cause the sensor to bend and change the backscatter signal which will act as the indication that a certain temperature has been reached (Khan et al. 2021). The current research found has developed sensors to detect -30° to 100°C (Caizzone et al. 2011; Khan et al. 2021). These are innovative solutions to temperature sensing, however, they do rely on visible and open spaces to best see and read the sensor. If the required amount of space is provided, or they can be easily viewed after a high-temperature event, then these sensors would be very beneficial. These sensors do need to be visibly accessible, so either keeping them in plain view or in an easy-to-access area will be the most efficient.

2.3 RFID-Based Sensing

Radio Frequency Identification (RFID) is a wireless sensing system that is commonly used as an asset monitoring system due to its low cost (Franchina et al. 2019). However, it can also be used for a variety of sensing applications, such as temperature, and humidity sensors if set up properly (Abdelnour et al. 2018; Hamrita and Hoftacker 2005; Zhang et al. 2017). RFID is split into three general systems: active, passive, and semi-active. All three of these systems will allow for health monitoring if a sensor or other means are used with the tag (Hamrita and Hoftacker 2005). Active and semi-active are battery-powered. Active systems utilize the power

for sensing and communication and can store information in between readings. Semi-active tags use the battery solely to power a sensor (Caizzone et al. 2011; Occhiuzzi et al. 2013). On the other hand, passive tags can only transmit information at the time they are powered by the reader because they do not have a battery (Babar et al. 2012a; Occhiuzzi et al. 2013). To receive constant data from a passive tag, a reader must be able to continually transmit signals to the tag and then returned data from each reading is recorded, otherwise referred to as a continuous-wave system (Abdelnour et al. 2018). Passive UHF RFID systems are preferred for asset tracking due to their long-read ranges and high reading rate, and depending on the tag, passive systems can be more cost-effective than active or semi-active systems (Franchina et al. 2019). Due to the lack of battery in a passive RFID tag, they do tend to live longer than their active and semi-active counterparts.

Active and semi-active tags are easier to configure for structural health monitoring and can store data with more ease than passive systems, but they do require more frequent replacement due to the limited battery life. A passive system can still be used as a structural health monitoring system when set up correctly (Hamrita and Hoffacker 2005). The use of chemically interactive materials in a tag can allow volatile chemicals to be detected by RFID sensors, passive RFID tags included (Amendola et al. 2014; Hamrita and Hoftacker 2005). Alternatively, integrated circuits can be added to RFID tags to allow for system monitoring, such as temperature readings. For examples, the combination was used to monitor the temperature of concrete during the curing process (Liu et al. 2017). The sensing capabilities and the read range of an RFID tag are inversely related, as the chemical or physical changes exerted on the tag change the energy that the tag can release (Occhiuzzi et al. 2013).

2.4 RFID Read Range

The read range of an RFID tag and the strength of its backscatter signal can be affected by the properties of surrounding objects (Occhiuzzi et al. 2013). In free air, an RFID system can have long, undisturbed read ranges, however, materials such as soil, metal, water, or moisture can reduce the read range and backscatter signal strength (Abdelnour et al. 2018; Bauer-Reich et al. 2014; Franchina et al. 2019; Huang et al. 2020; Mishra et al. 2014; Vyas and Tye 2019). From previous research, increasing the water content of soil increased the attenuation of RFID tags, however, magnetic fields from RFID tags are not impacted as strongly (Vyas and Tye 2019). Concrete, and more specifically wet concrete, can limit the read range of tags, and metal can detune RFID tags, if they are not properly designed and implemented (Abdelnour et al. 2018; Babar et al. 2012a; Franchina et al. 2019; Hauser et al. 2005; Vyas and Tye 2019; Liu et al. 2017).

The read range of an RFID tag also depends on the tag antenna's geometry and the substrate of the antenna (Babar et al. 2012a; Babar et al. 2012b). The performance of the RFID tag is directly related to the size of the RFID tag antenna, as the antenna gets larger, the performance gets better, and vice versa (Babar et al. 2012a). However, the antenna can be sized down if a substrate with a higher permittivity value is used beneath the tag; these substrates can also be flexible, allowing RFID tags to be placed in smaller, not flat, cavities (Babar et al. 2012a; Franchina et al. 2019; Hauser et al. 2005; Liu et al. 2017).

The RFID system that is chosen can also influence the read range. Active tags have a battery and can use that power source to send a signal, which leads to a higher operating range than passive tags. Passive tags send signals back based on the limited power sent from the reader (Reinisch et al. 2011). As mentioned previously, if a short-term monitoring system is needed,

then active tags may be the solution, but if longer-term monitoring is required, the continual replacement of active tags can be a limiting factor due to cost.

2.5 RFID Temperature Sensing Systems

Understanding how RFID tags change when close to certain mediums can allow for innovative temperature sensors (Aroca et al. 2018). Bhattacharyya et al. (2010) developed a cold storage temperature threshold sensor that utilized the understanding of how tag performance changes when exposed to water (Bhattacharyya et al. 2010). This system used two tags separated by a thin layer of ice, when the threshold is exceeded, the ice melts onto the bottom tag, rendering the bottom tag useless (Bhattacharyya et al. 2010). When the system is read, the missing signal from the bottom tag alerts users that the transported goods may not be safe anymore. Separately, Virtanen et al. (2011) used distilled water as a sensing element along with an RFID tag over an operating temperature range of 0°C to around 100°C. They considered how distilled water changed when exposed to certain temperatures and looked for a change in the backscatter signal to determine the temperature change (Virtanen et al. 2011).

The use of shape memory alloys can also alter some tag properties, such as the reading frequency, which can then be used to determine the temperature. Khan et al. (2021) looked at attaching RFID tags to shape-memory alloy beam, which would bend when exposed to 50 °C for 30 seconds; when bent, the backscatter strength of the tag would decrease. Another development of RFID tags with shape memory alloys was implemented by Caizzone et al. (2011). They used two microchips, one that would read no matter the temperature, and second that would transmit based on the temperature. Different shape memory alloys would cause the RFID tag antenna to bend at different temperatures. This results in a system that could be designed to sense temperatures from -30°C to 100°C, with a read range of around 30 mm. Currently, a fully passive

temperature sensing RFID system is limited to 100°C, but there is potential to reach higher temperatures.

2.6 RFID Sensors in Underground Systems

RFID systems that are implemented in soil do need to consider the loss of signal strength caused by the moisture in the soil. Active systems can be a solution, but if a long-term sensor system is needed, an active system may not be the most cost-effective (Aroca et al. 2018, and Reinisch et al. 2011). Several authors have presented or developed different equations to estimate the signal path loss of wireless sensors in the soil, but the variability of soil conditions does make it difficult to get an accurate answer (Abdelnour et al. 2018; Huang et al. 2020; Reinisch et al. 2011; Sing et al. 2009). The use of RFID in mining operations is also being looked at, but the corners in mines can limit signal propagation and make it difficult to read every signal tag (Mishra et al. 2014). Another factor to consider is the movement of the soil. When people, animals, or even machines move across the ground, the soil can shift which can potentially damage any exposed wirings or fragile components of the sensor (Aroca et al. 2018).

One solution to the signal loss that occurs in the soil is to use multiple nodes with increasing depth in the soil (Lin et al. 2019; Sing et al. 2009). The idea is that one node receives the signal from the reader, which then is programmed to propagate the signal down to the next node, and the cycle repeats until the signal gets to the last node. The signal is then sent back up the chain and to the reader to gain the information from the sensor nodes. Lin et al. (2019) found that this system could be powered continuously for 27 days, or up to 2 years if the data reporting occurs once every hour.

If a passive system is preferable, comparing the necessary input power for the tag and the output power of the reader chosen will give a decent idea of the potential read range; the greater

the difference in power, the higher the operating distance (Reinisch et al. 2011). However, this doesn't fully account for the loss of signal due to soil moisture, so that will also need to be considered. UHF passive systems are preferable for underground applications as they have a frequency that can potentially reduce loss from the soil (Abdelnour et al. 2018). One subsurface sensor design uses a frequency doubler to make up for any signal loss going back to the reader, and the reader would process that information, eliminate any extraneous data and read the tag (Abdelnour et al. 2018). This setup allowed for a read range of up to 60 cm under the soil with a 25% or less water content (Abdelnour et al. 2018).

Beyond just considering it as a limitation, the impact of soil moisture on RFID tags response was leveraged to detect the moisture content in the soil. Passive soil moisture monitor sensors were developed by Aroca et al. (2014); they placed 3 sensors during testing, at 5, 15, and 20 cm below the surface, and were able to receive signals from the tags to a reader placed just slightly above the surface. Using a similar ideology, Bauer-Reich et al. (2014) looked at how the depth of a sensor and the moisture connection impacted the read range. When their system was placed in soil, they found a read range of around 2 m, with the tag at a depth of 15 cm.

Chapter 3. Background

RFID-based wireless sensing systems are commonly used for asset monitoring, keys, and race timers. There are four main parts to an RFID system: the reader, the antenna, and the RFID tag. The RFID reader will send a signal through the antenna, to tags within the system's read range. The RFID tag itself is comprised of a tag antenna, which will catch and return the signal, and an RFID chip. The chip is where the tag's identification number and any information stored on the tag will be found. The signal is sent to the tag chip and then sent back to the reader for information to be collected and stored. These main components dictate the read range, durability, and cost of the system operation.

The reader, or interrogator, is the main component of an RFID system. This device, either fixed or handheld, sends and receives signals from the entire system of tags. A fixed reader needs to be connected to a power source, which allows the use of stronger signals. These fixed devices are more commonly used in warehouses for asset tracking in large spaces, as their signal can reach further distances. Handheld readers are smaller and more portable, even cell phones can become RFID readers if the correct app is downloaded. However, because handheld readers only have a limited power supply, tags need to be relatively close for the reader to register. Handheld readers are often used for key-type applications such as for hotel rooms and apartments.

Antennas are used to convert the RFID reader's signal into RF waves, which RFID tags can register. The polarity of the RF waves sent out by the antenna is either along horizontal or vertical planes. Similar to other wireless systems, if the polarity of the antenna matches the polarity of the RFID tag, the read range of the system can be longer than if they mismatch. Circularly polarized antennas transmit waves in both the horizontal and vertical planes. This antenna is beneficial if multiple tags are used with different polarities. The signal from circularly

polarized antennas is rotated between the horizontal and vertical planes, and because the energy is divided among the two planes, the reader range will be shorter than that of a linear antenna.

Two reader and antenna combinations are possible: an integrated system and a separate antenna and reader. When an integrated RFID is used, the antenna is built into the reader. If the antenna is distinct from the reader, an antenna port and a cord are used to connect the antenna and reader. The thickness and length of the cord can impact the read range of the system with a longer and thicker cord causing a shorter read range than a thinner and shorter one. However, the influence of the cord choice on the read range is not as impactful significant as the reader or antenna design.

RFID systems operate within 3 different frequency ranges, which are generalized as low frequency, high frequency, and ultra-high frequency (UHF). Low-frequency systems are typically used for car key fobs and animal tracking and work well near liquids and metals. However, they do have a shorter read distance and a high production cost. High-frequency systems are typically used for library books, and personal ID cards and have larger memory options than the other two frequency ranges. The read distance of high-frequency systems is short with a low data transmission rate. UHF systems can be broken into active, semi-active, and passive RFID. Active tags are equipped with a battery and can store data between readings. These are typically used for vehicle tracking, mining applications, and asset tracking. Semi-active tags are similar, except the battery is used to power a connected sensor system. Both systems have large memory capacities and can track and store information between contact with readers. Due to the battery, they have a long-read range, but they generally have a much shorter life span than other tags. Passive RFID is typically used for supply chain tracking, manufacturing, and race timing. Passive systems cost less per tag when compared to active systems and have a wider variety of shapes and sizes of

tags. However, they only have a moderate memory capacity and a shorter read range than active tags. Proximity to water and metals can cause interference in RFID systems in the high frequency and UHF range.

Chapter 4. Sensor Design

The goal of this research is to develop a system that communities can use after wildfire events to find potential areas of contamination more efficiently in the water distribution system. Two potential causes for the contamination are the heating of the service pipeline materials or negative pressure within the system that causes backflow in the system and allows contaminated gases into the system (Schulze and Fischer 2021). The sensor system presented herein is developed to address the heating of polymer-based pipes as a source of contamination. First, the key design considerations developed from previous work and wildfire findings are outlined. Second, the proposed sensor solution is presented.

4.1 Design Considerations

Based on the previous wildfire experiences and work in pipeline monitoring outlined in Chapters 1 and 2, the following considerations were used when developing these sensors:

- *Buried Wireless system* – Systems with components on the ground surface have the potential to fail prematurely due to the high temperatures. Further, the temperature of the wildfire might vary significantly from the ground surface to the buried depth of the pipeline based on fuel load, duration, and soil type. A buried, wireless system allows for everything to exist right at the pipeline and offers protection for the sensing system.
- *No Internet access required* – Although wireless, the sensors should have the capability of being read without the use of the Internet. Recently, in the Boulder fire in Colorado, the internet was not readily available (Whelton et al. 2023). In case this happens in future wildfire events, these sensors should still be usable.

- *Cost-effective, Easily Deployable* – Often the regions impacted by wildfires and the water pipeline networks are large, so sensors costs should be low to allow for dense deployments and encourage adoption.
- *Longevity of the sensor* – These sensors should have a long lifespan. Forest fires do not occur at regular intervals, so using a system that only lasts 5 years would be inefficient and would cost more money as the sensors would need to be replaced.

Given these design considerations, RFID-based sensors seem best suited to the application. They are wireless systems that can be read without the internet, relatively cost-effective, and all can be used as temperature sensors if properly designed. RFID tags are not large, therefore the implementation of them underground only consists of one hole big enough for an RFID system, and deep enough to monitor the selected systems. A passive RFID system will be more likely to achieve a long lifespan, currently, passive RFID systems can survive around 30 years. Thus, a passive RFID system achieves the five objectives listed above.

The depth at which these sensors should be placed is dependent on how the soil responds to heat, as well as the read range of the sensor. Research from Metz et al. (2022) has found that the heating threshold for PVC and HDPE pipelines to leach VOCs are 194 and 250°C for 30 minutes, respectively. To determine at what depths these thresholds will occur, analytical models for soil temperature profiles were developed by Richter (2021). The threshold depth will change depending on the surface heat flux of the wildfire and the duration of the wildfire. For a heat flux of 15 kW/m^2 at 2 hours, temperature greater than 194° C occur from the surface to a depth of 0.12 m (4.3 in), and greater than 250° C occurs from the surface to a depth of 0.1 m (3.9 in). In a wildfire with a heat flux of 30 kW/m^2 for 2 hours, the PVC threshold will occur from the surface to a depth of 0.18 m (6.5 in), and the HDPE threshold will occur from the surface to a depth of

0.16 m (5.8 in). Currently, there are two main pipeline depths, the depth to the service line, 0.5 m (18 in), and the depth of the water main, 3 m (9 ft). However, the service lines ultimately need to reach the structure, so their depth may vary. Based on the analytical models from Richter (2021), the critical depth of the pipeline will be from the surface to around 0.2 meters.

Ultimately, the number of sensors deployed in a community will depend on how many pipelines that are within the threshold depth, budget, and risk tolerance of the community. Keeping costs and maintenance efforts low should enable potentially dense deployments.

4.2 Sensor Design

A passive RFID-based system will be used, but a passive RFID tag cannot track and record temperatures while a forest fire is occurring, so an alternative system will be needed. Bhattacharyya et al. (2010), Caizzone et al. (2011), and Khan et al. (2021) all discussed a passive system that considered how RFID tags interact with surrounding materials to measure a threshold temperature. Bhattacharyya et al. (2010), separated two RFID tags by a thin sheet of ice, once the threshold was reached the ice would melt onto the tag on the bottom, stopping the bottom tag from transmitting a signal. Both Caizzone et al. (2011), and Khan et al. (2021) used shape memory alloys, which would bend at a specified temperature, to cause the signal of the RFID tag to be weaker. The passive temperature threshold sensors only have an operating range of up to 100°C, which will not be sufficient for wildfire events, but they do offer inspiration for this pipeline temperature sensor system. A material that would melt at the heating threshold of each pipe could be used to stop a passive tag from reading, alerting any users to test the water.

If only one RFID tag is used within the system, there is a high likelihood of false positives that indicate the threshold is reached. Temperature sensors designed and discussed by Bhattacharyya et al. (2010), and Khan et al. (2021) both used two-tag passive systems as

temperature threshold sensors. Each had one tag that would read regardless of the temperature exposed to the system, while the other tag would only read until a temperature threshold has been reached. The use of a read-only tag and a threshold temperature tag was a big influence on the design of these sensors. If only a temperature threshold tag was provided, it may be hard to determine if a particular pipe was affected. The use of the second tag means that sensor systems could be localized, and the threshold condition effectively identified.

In this paper, two different models were developed and tested, Model 1 (M1) and Model 2 (M2). Both sensors used the same RFID reader and antenna system as shown in Figure 4.1. Both sensors use a similar framework of RFID sensors and enclosure but implement a different threshold circuit design. Each used a Digi-key Molex RFID tag for the threshold temperature sensor and a high-temperature Model C2525 passive RFID tag from RFID Inc. The Molex RFID tag is listed to have a read range of 4.5 m and has direct access to the tag's antenna (Molex 0133580821). The C252 high-temperature tag is encased in ceramic to survive up to 250°C and has a shelf life of about 40 years (RFID Inc). They system is protected within a rectangular alumina (Al_2O_3) crucible will be used; anything moving over soil can disturb and shift the soil around the sensor system, so any exposed elements could be compromised. Every RFID tag has an ID number to distinguish them from each other. Each type of tag has matching values for the first 8 digits of its ID. Therefore, the Molex tag and High Temperature tag can be identified while in the ground. To prevent this, and to give the system a small amount of protection a rectangular alumina (Al2O3) crucible will be used. The crucible is 100 x 40 x 20 mm in size to fit the high-temperature tag which is 25 x 25 x 3mm.

Figure 4.1: RFID system Set-up

The central difference between the two models is how the threshold sensor is designed. The baseline for both is that a circuit-based system will be incorporated into the antenna of the Molex tag, which is shown below in Figure 4.2. A cut will be made in the antenna to alter the RF wave signal, and the circuit will be added to the antenna at that cut point. The cut point for each Model was chosen to best fit the threshold circuit designed.

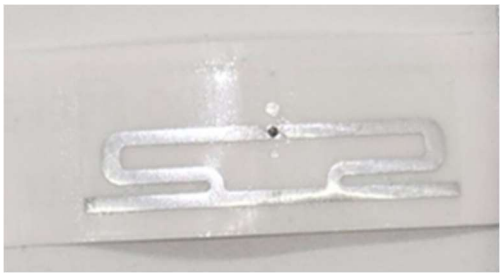

Figure 4.2: Molex Tag

The design of M1 is shown below in Figure 4.3. The overarching idea was for the circuit to act like a switch. There are two rods in M1, the pinned and the fixed rod, that act as the circuit. Copper wires are soldered to the brass rod and then connected to the antenna with tape at the cut. The wire used must be conductive and have a coating that can withstand high temperatures, otherwise, the wires could damage the rest of the sensor. A trigger material supports the pinned

rod to stay up and was chosen to melt at the threshold, such that the pinned rod would fall to break the circuit. Before the threshold is reached, the circuit will be closed, and the RFID tag will be able to send a signal to and from the RFID chip, because the antenna is closed. When the threshold is reached, the circuit will open and because the antenna is no longer closed, the signal should not be able to effectively propagate to the RFID chip of the tag or back to the reader. In both cases, the high-temperature tag will always read and will indicated the pipe's locations and limit false positives.

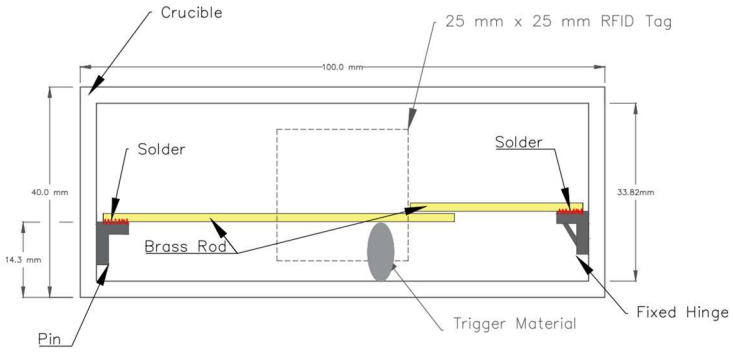

(a) Front View

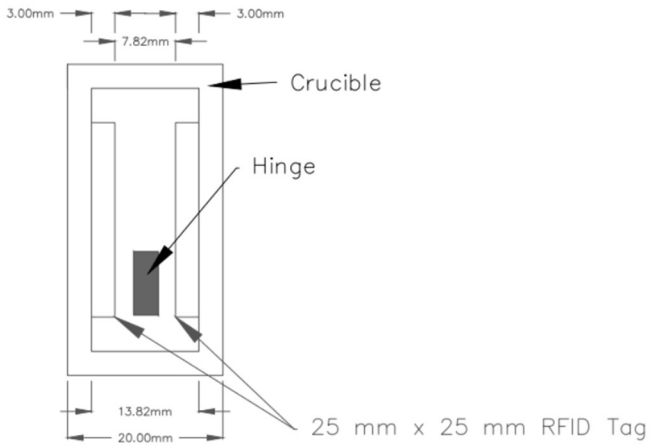

(b) Side View

Figure 4.3: Model 1 Design: (a) Front View, (b) Side View

To ensure that the system layout would only trigger due to the change in the trigger material as intended, the displacement of each rod was calculated considering the dimensions, self-weight, and material properties under heat. The material properties of the rods, including the self-weight (w), the modulus of elasticity at room temperature (E_0) the moment of elasticity at 194°C (E_{194}), and the moment of inertia (I). The moment of inertia depends on the shape of the rod; a hollow rectangular rod was used for M1. The outer width (w_1) and height (h_1) and inner width (w_2) and height (h_2) of the hollow rod was used to find the moment of inertia as

$$I = \frac{w_1 * h_1^3 - w_2 * h_2^3}{12} \quad \text{4-1}$$

The deflection of the fixed rod can be approximated using the self-weight, length, modulus of elasticity, and moment of inertia as.

$$d_f = \frac{w * L_f^4}{8 * E * I} \quad \text{4-2}$$

where L_f is the length of the fixed rod. The deflection of the pinned rod is dependent on the change in height of the trigger material. The height of the pinned support (H_p) will limit the deflection that the pinned rod can undergo. Using similar triangles, the deflection of the pinned rod due to the difference in height between the pinned support and the height of the trigger material can be calculated. The distance horizontally from the pinned support to the center of the support and the vertical difference in height will serve as the first triangle. The unknown vertical displacement of the pinned rod, d_p is

$$d_p = L_p * \sin\left(tan^{-1}\left(\frac{d_0}{x}\right)\right) \quad \text{4-3}$$

where L_p is the length of the pinned rod, d_0 is the difference in height between the pinned support and the trigger material and x is the horizontal distance from the pinned support to the center of the trigger material. The displacement of the pinned rod should be greater than the displacement

of the fixed rod to fully break the circuit. Making the fixed rod short, around 20 mm, will limit the vertical displacement, and placing the height of the fixed and pinned rod above the displacement range of the fixed rod will ensure the circuit breaks as intended.

Model 2 is a simpler version of M1; the design is shown below in Figure 4.4. Instead of using wires, rods, and hinges, M2 just uses the trigger material to compress a metal plate and complete the circuit. The cut in the RFID antenna is on the side and a brass plate is placed over the cut to close the antenna. The use of a plate means that once the plate is removed only the tag antenna with the cut is left, ensuring that the Molex tag will not read effectively. The trigger material will be used to keep the plate pressed against the tag, which will be placed at the top of the box. The trigger material is epoxied to the plate, and when the trigger material melts, the plate will fall away from the antenna, breaking the circuit.

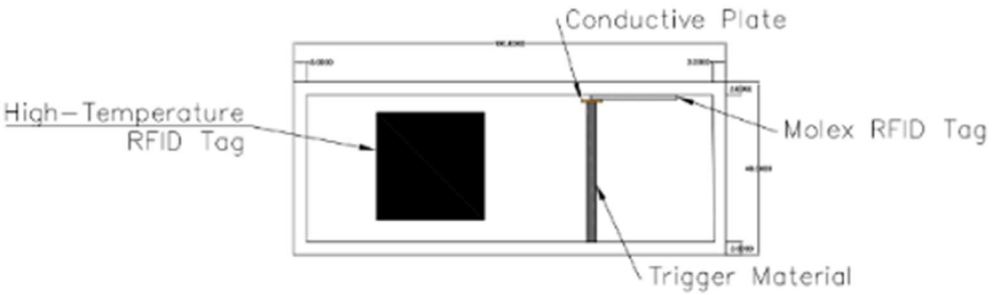

(a) Front View

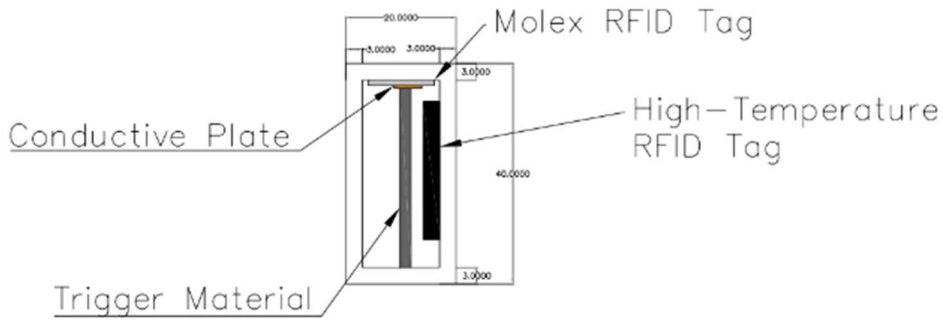

(b) Side View

Figure 4.4: Model 2 Design: (a) Front View, (b) Side View.

The key advantage of M2 over M1 is the simplicity in design, which improved reliability and makes it easier to set up and replace. If the hinges in M1 are not properly secured, the connection could fail and the leftover residue from the epoxy makes it difficult to reuse the crucible later. Epoxy can prevent the hinge from moving properly if not applied well, which can prevent the system from working as intended. Finally, M1 has more moving parts, which have more potential for failure, while M2 is very easy to set up and change if necessary.

Both models utilize a trigger material to open the antenna. The trigger material was chosen by comparing various materials' melting points, cost, and the threshold temperature for each system. PVC, Nylon-12, and HDPE plastic have melting points of 170 – 210°C, 190 – 200°C, and 210 – 270°C, respectively. The dimensional changes of each material at the threshold

helped determine how to set up M1 to ensure the system triggers at the correct time. Changes in the height of the trigger material dictate how far the pinned rod in M1 would drop, so two heights were proposed for the PVC and HDPE, ~5 mm and ~15 mm. Each trigger material was cut into small pieces and their height, width, and thickness were recorded. The PVC tested was small portions of PVC pipe, which have a maximum working temperature of 60°C (140°F) ("1/2 in. x 24 in. PVC Sch. 40 Pipe,". *Home Depot*). A maximum working temperature of 82.2°C (180°F) is given for the HDPE pipes ("Marine-Grade Moisture-Resistance Polyethylene (HDPE) Sheets and Bars," *McMaster-Carr*). The Nylon—12 has a maximum working temperature of 93.3°C (200°F) ("Long-Lasting Cable Ties," *McMaster-Carr*).

Once each piece was measured it was placed upright inside the alumina crucible, as shown below in Figure 4.5, and a lid was placed on top to replicate the environment the material would experience in the sensor system. The crucible was placed in the oven at room temperature, and the oven was set to heat up to the threshold temperature and hold that temperature for 5, 10, 20, and 30 minutes. Once the time was met, the heater was turned off, and the crucible was removed from the oven. The pieces were allowed to cool and were then measured, and the average of each measurement was recorded. The differences in height before and after heating is shown below in Figure 4.6 as a percentage with the maximum and minimum changes shown. Each material was tested 3 times per height for 5, 10, 20, and 30 minutes, resulting in 12 tests total for HDPE and PVC each at ~5mm and ~15mm.

Figure 4.5: Trigger Material Oven Set-up Without Crucible Lid

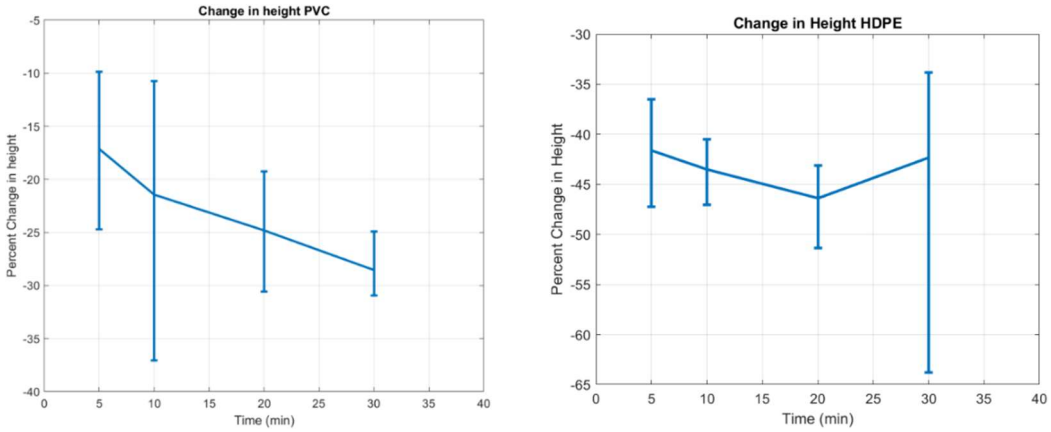

Figure 4.6: Average Height Change for PVC and HDPE

The change in height for PVC is more predictable than that of HDPE and tracks the duration of heating, but the HDPE material height does change more significantly with heating. The large error bars could be due to using two different ovens that may have slightly different heat fluxes, the time each specimen sat in the oven could have varied slightly between tests due to human error, or the lid was not secured well, and the heat transfer into the crucible was faster.

Nylon—12 zip ties were used as test specimens due to their small melting point range. However, because of the limited thickness of the specimens, all the Nylon—12 samples did melt to the bottom of the crucible after heating, as seen below in Figure 4.7. If the time of threshold

time is determined to be very short, Nylon—12 may be a good alternative to PVC and HDPE. Oven tests have not been conducted to look at dimensional changes of thicker Nylon 12 samples.

(a) Before Heating (b) After Heating

Figure 4.7: Nylon 12: (a) Before Heating, (b) After Heating

Chapter 5. Sensor Testing and Results

Two different testing methodologies were used to evaluate the proposed sensor models: benchtop testing and testing in a more realistic environment. Benchtop testing includes oven tests and hot plate tests. A soil box was used to perform tests in a more realistic environment. The goal of all these tests is to find how the sensors perform under varying environments and propose improvements.

The main set of tests performed were oven-based benchtop tests to establish the soundness of the approach. The soil box and hot plate tests were conducted to place the sensors in a more realistic environment and expose them to their designed threshold temperature to see if they work as intended. The oven and hot plate tests were performed at the University of Minnesota Twin Cities, while the soil box tests were performed at Oregon State University. The soil box and hot plate tests are similar, with the hot plate tests being a smaller version of the soil box tests, which could be done at a benchtop scale with less overall effort.

For example, to determine if a circuit could be added to an existing RFID tag antenna, cuts would be made to the antenna while the RFID reader is sending signals. A small section of the tag antenna would be removed, as shown in Figure 5.1, and the signal would stop propagating. The conductive material, such as copper wire, would be placed at both ends of the cut to determine if the signal could read. These tests were just to confirm the theory that a circuit could be added directly into the antenna and that the opening and closing of the circuit would cause the tag to function as desired.

Figure 5.1: Cut RFID Molex Antenna

5.1 Oven Tests

Oven tests provided a controlled environment in which to establish a baseline for the sensors. After the sensors were completely built, the tags were read to note what the identification number of the RFID tags for the test. The circuit was either opened for M1 or removed for M2 to determine if the Molex tag is working as intended before starting the test. Once there was confirmation that both tags work, the lid was added, and high-temperature tape was used to seal the system. The sensors were placed in the oven at room temperature to best replicate the environment before a wildfire event, and the oven was set to heat up to the threshold temperature based on the trigger material used. The threshold temperature was held for 30 minutes, and the sensor is removed from the oven once the oven has cooled back down to room temperature. The reader was set to run, and it was noted which of the two RFID tags is reading was noted. If M1 was being tested, the sensor was be left and would be read again in 24 hours.

After the tests were done, the lid was removed, and the internal working of the system viewed. If the Molex RFID tag was read after testing, seeing the circuit after heating can give hints as to why the system didn't work. The pre- and post-heating for M1 and M2 for the oven tests are shown in Figure 5.2 and Figure 5.3, respectively.

(a) M1 Pre-heating (b) M1 Post-heating

Figure 5.2: Pre and Post Oven test for M1: (a) M1 Pre-heating, (b) M1 Post-heating

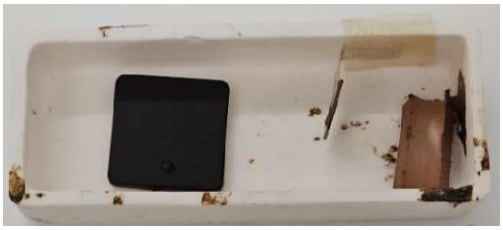

(a) M2 pre-heating (b) M2 post-heating

Figure 5.3: Pre and Post Heating for M2: (a) M2 Pre-heating, (b) M2 Post-heating

Three oven tests were conducted for M1, referred to as M1o1 through M1o3, where the 'o' in the naming convention indicated the type of test. The setup prior to heating for each is shown in Figure 5.4. M1o1 just had the Molex tag connected to the circuit by the wires only, there was no support to keep the tag in place. M1o2 used the same circuit system and tags as M1o1 but a piece of tape was used to hold the Molex tag against the lid to ensure that the trigger material was the only reason the Molex tag would not read. M1o3 used a new set up, which better reflected the angles at which the hinges would fall on their own. The trigger material was cut and placed in a way to support the rod at the point of free fall.

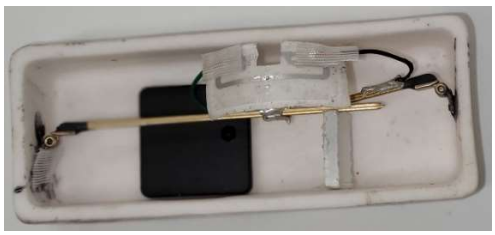

(a) M1o1

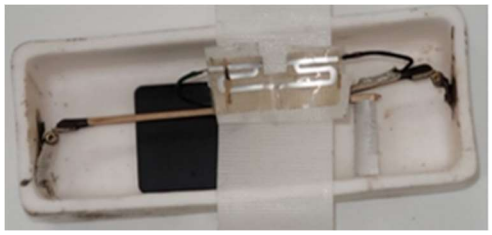

(b) M1o2

(c) M1o3

Figure 5.4: M1 Oven Test Setups Prior to Heating: (a) M1o1, (b) M1o2, (c) M1o3

After the oven test, M1o1 was the only setup that properly trigger - only the high-temperature tag was reading. However, when looking inside the box, the Molex tag disconnected from the circuit sometime during the heating process, which lead to the Molex tag not reading. Although this sensor did have the wanted results, it did not work as intended and there was no way to tell when the tag disconnected from the circuit during these tests. M2o2 after heating saw both tags being read; the system was left for 24 hours to let the system cool fully, and both tags were still reading. After looking inside, the box, the trigger material did burn and shrink as designed, but the pinned rod was still horizontal. M1o3 had the same result, the Molex tag was still being read. In this case, the trigger material did shrink, and the bars did separate, but they did not separate enough to stop the signal from reaching the RFID chip. The results for each setup are shown in Figure 4.6.

(a) M1o1 Oven Results

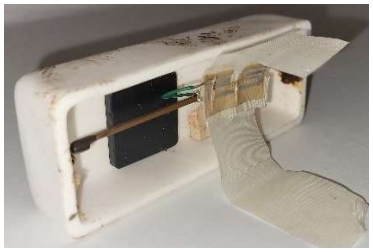

(b) M1o2 Oven Results

(c) M1o3 Oven Results

Figure 5.5: M1 Oven Test Results: (a) M1o1, (b) M1o2, (c) M1o3

For both M1o1 and M1o2, the hinges have a limited rotational range. There may be two main causes for this: 1) Epoxy was used to adhere the hinge to the wall of the crucible. If any epoxy gets into the barrels, the hinge can be made useless and permanently fixed at the angle the hinge was at when the epoxy dried. 2) The heat could be unevenly expanding parts of the hinge, which would hinder rotation as well. Even in M1o3, there was only a limited amount of rotation, even though the trigger material is out of the way of the pinned rod.

Oven tests for M2 were conducted for both PVC (M2oP1 and M2oP2) and HDPE triggers (M2oH1, M2oH2). For the PVC tests, different crucibles with different tags were used. For M2oP1, the conductive plate was epoxied to the trigger material, while M2oP2 just used pressure from the trigger material to keep the conductive plate in place. The sensing systems, M2oP1, and M2oP2, prior to heating are shown in Figure 5.6. The HDPE test setups were similar. Each test was conducted with different crucibles and materials; however, no epoxy was used

between the trigger material and conductive plate. The setup for M2oH1 and M2oH2 is shown in Figure 5 8. M2oH1 did use the same crucible as M2oP2 and the same Molex tag; if the Molex tag survived a test, it is usable for another.

(a) M2oP1 (b) M2oP2

Figure 5.6: M2 Oven Test Set-up: (a) M2oP1, (b) M2oP2

(a) M2oH1 (b) M2oH2

Figure 5.7: M2 HDPE Oven Test Set-up: (a) M2oH1, (b) M2oH2

After heating the Molex tag did not read for either M2oP1 or M2oP2. Both trigger materials worked as intended, the main difference being how the plate was affected. The trigger material for M2oP1 did pull the conductive plate down, making the Molex tag inoperative as designed. For M2oP2 the conductive plate was stuck to the adhesive side of the Molex and just bent the Molex tag in a way to make it inoperative. The results from the oven test for M2 are shown in Figure 5.8.

(a) M2oP1 results (b) M2oP2 results

Figure 5.8: M2 Oven Results: (a) M2oP1 results, (b) M2oP2 results

Both HDPE tests for M2 supplied the same results: the high-temperature tag was the only one that was reading post—heating. When HDPE starts to melt, the material becomes very adhesive which caused the conductive plate to stick to the trigger material instead of the tag without epoxy and the conductive plate was separated from the tag antenna, as shown in Figure 5.9.

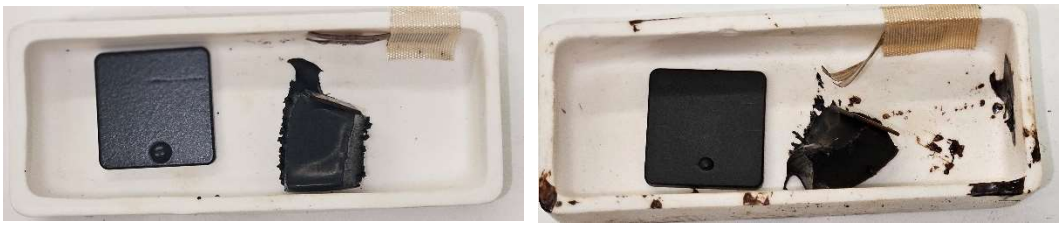

(a) M2oH1 (b) M2oH1

Figure 5.9: M2 HDPE Oven Test Results: (a) M2oH1, (b) M2oH2

While the tackiness of the HDPE when exposed to high temperatures can be advantageous, in M2oH1, the trigger material got stuck to the back of the crucible, making the system hard to reuse. This did not happen in M2oH2, however. When cutting the trigger material, it may be helpful to cut a thinner piece and place the piece, so it does not touch the back or front of the crucible, to aid with reusability. Alternatively, the crucible can be placed back in the oven to reheat the material, and before the material has cooled, carefully remove the piece to reuse the

system. It may also be helpful to place a small amount of epoxy on the conductive plate to ensure that the trigger material and plate move together.

Overall, M2 is much simpler than M1, but with the downside that once the trigger material melts, the Molex tag will stop reading, and the system could trigger too early. However, M2 is much more consistent with triggering at or around the threshold than M1. M2oP2 does show that if the conductive plate is not epoxied to the trigger material, the plate can stick to the adhesive of the Molex tag. Finally, the trigger material does need to be cut with more precision for M2, if it's too short and epoxy is used, the plate may not have enough pressure to complete the RFID antenna tag.

5.2 Soil Box Tests

Soil box tests were aimed to create a more realistic environment that mimics what the sensors might experience. The soil box will supply one direction heat flow for the sensors, which better represents the heat the sensors will experience during a wildfire. These tests were performed at Oregon State University. The soil box was made using a deep rounded steel trough with fiberglass insulation placed against the inside of the trough. Soil from outside the lab in Corvallis, Oregon State University was used to fill the soil box. A few inches of soil were placed and compacted before the PVC or HDPE pipe samples were placed inside. The identification number of the tags used was recorded and their placement was noted. The sensors are placed on top or the side of the pipe samples, as seen in Figure 5.10, and two additional lifts of soil were placed and compacted over the pipes and sensors. Ceramic rods were placed near each pipe with thermocouples at 2-inch increments to monitor the heat change the soil experiences. Once the soil was fully compact, the RFID reader was turned on to ensure that all the RFID tags were still readable. A rack with two square heaters (referred to as North and South) were then placed over

the soil box, and the heaters were lowered so they were on top of the soil, and any open space was filled with fiberglass insulation to limit any heat from escaping. The same base setup was used for both PVC and HDPE testing; the pipe samples were changed, and the critical temperature was adjusted to correspond to the threshold found for each pipe. The heaters were designed to heat the soil until the temperature at the depth of the pipes equals the threshold and then the heaters held that temperature for 30 minutes. Once the heating was complete, the heaters were turned off and the soil box was left overnight to cool. In the morning the sensors were read to determine if the threshold sensor had triggered, and then the soil above the pipe and sensor were removed to check the status of the pipes and sensors.

(a) M1sbP Test (b) M2sbH Test

Figure 5.10: M1 Soil box set-up (a) M1sbP test, (b) M1sbH 1-7 test

Currently, only M1 with PVC and HDPE has been tested with the soil box. For the PVC tests, two sensors were deployed, M1sbP1 and M1sbP2. Both sensors used PVC as a trigger material, but each used a different wire to connect to the circuit. The sensor under the North heater, M1sbP1, used 20-gauge solid copper wire, while the sensor under the South heater,

M1sbP2 as shown in Figure 5.11, used 24-gauge threaded wire. These sensors were placed on top of the pipe samples and secured with high-temperature tape as shown in Figure 5.10 (a).

Figure 5.11: Set-up for Soil Bix Testing

During testing for M1sbP, the South heater was not emitting the amount of heat necessary to heat the South pipe to the threshold temperature, but the North heater was. As a result, the South sensor, M1sbP2, was assumed to still have both RFID tags reading, while the North sensor, M1sbP1 would only have the high-temperature tag reading. After testing, however, all four tags were still reading. While digging up the soil, the North sensor was damaged and the soil got into the box as shown in Figure 5.12 (a), so the failure to trigger is not clear. The trigger material for the north sensor worked as intended, but the pinned rod did not fall, leaving the circuit closed. The wires connected to the Molex tag for the North sensor, M1sbP1 disconnected from the Molex tag, but it was not clear if this happened before or after the crucible was damaged. The South sensor, M1sbP2, looked completely intact after testing. The trigger material did not shrink as seen in Figure 5.12 (b), so the temperature reached the South heater was likely not close to the threshold temperature.

(a) M1sbP1

(b) M1sbP2

Figure 5.12: M1 PVC Soil Box Test Results: (a) M1spP1, (b) M1sbP2

For M1sbP1, the thicker wires could have held the pinned rod in place. They were not very flexible, and in some instances, closing the lid caused the epoxy to fail and the hinge to break off from the wall. The hinges were stiff and did not have much rotational capacity after heating; Similar to the oven tests, it is possible that epoxy got into the rotational cuff of the hinge, or that the heat caused the hinge to expand in a way that damaged the rotational cuff. M1sbP2 displayed that the trigger material does work in the intended range and that the sensor will not trigger prematurely.

The HDPE tests used three sensors using the M1 design, M1sbH1, M1sbH2, and M1sbP3, as shown in Figure 5.13. M1sbH1 re-used the M1sbP2 crucible, just replacing the PVC trigger material with an HDPE trigger material. M1sbH2 used solid, 20-gauge copper wire to determine if the threaded or solid wire made a difference in the performance of the sensor when using HDPE as the trigger material. M1sbP3 also used solid, 20-gauge copper wire, except used PVC as a trigger material, to see if a larger change in height would allow the pined rod to fall further and confirm the trigger was effective when subjected to a higher temperature. The North pipe had M1sbH1 taped on top of the pipe, while the South pipe had M1sbH2 and M1sbP3 placed alongside the South pipe as shown above in Figure 5.10 (b).

(a) M1sbH1

(b) M1sbH2

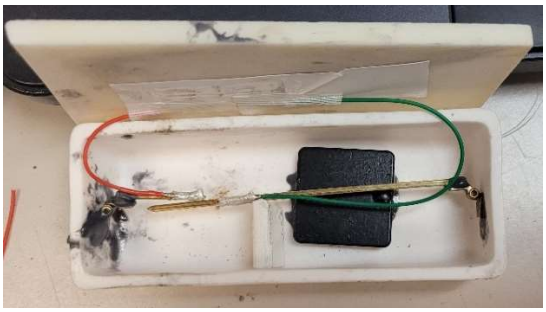

(c) M1sbP3

Figure 5.13: M1 Sensors for HDPE Soil Box Tests Set-up: (a) M1sbH1, (b) M1sbH2, (c) M1sbP3

During testing, one of the thermocouples was not working properly and was reading much higher temperatures at the depth of the pipe sample than the thermocouples at the height of the heaters. To be conservative, the lowest temperature at the depth of the pipe was used to track the temperature at the pipes. After the soil was allowed to cool, only 1 high-temperature tag was reading and none of the Molex tags were reading. The high-temperature tags being unable to read was unexpected as they are designed to withstand temperatures greater than 250°C. Upon looking inside the crucible, all the trigger materials were melted to the bottom. The pinned rod to M1sbH1, as seen in

Figure 5.14 (a), did fall as intended, but the fixed rod connection failed as well. This seemed to happen for all three sensors, which is why the Molex tag read for none of them; in general, the circuit failed, and the Molex tag and brass rods were burnt. Additionally, the wire

casings for all three sensors failed and left the wire exposed. The high-temperature tag casing has been slightly damaged in M1sbH1 and M1sbP3, as seen in

Figure 5.14 (b) and (c).

(a) M1sbH1

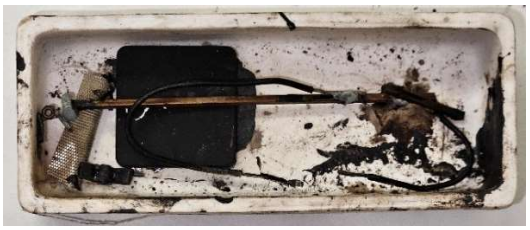

(b) M1sbH2

(c) M1sbP3

Figure 5.14: M1 HDPE Soil Box Test Results: (a) M1sbH1, (b) M1sbH2, (c) M1sbP3

Overall, the unexpected failures of the sensor system were likely due to the excess heat. In particular, the high-temperature tag casing failure could be due to excess heat, or the casings could have also failed due to proximity to the exposed wire and heated bars. A potential reason for the trigger materials melting as they did could be the residual heat from the soil; soil is a good insulator and will take longer than cool than air, so the additional time exposed to the high temperatures after the tests could be the cause. For future tests with M1, a wire with a high-temperature casing should be used to protect the wires and the materials around the wires. The epoxy used may need to be re-considered for epoxy with a higher temperature range, to ensure that the connections don't fail. Another material for the rods could be considered to prevent them

from heating the surrounding components. Finally, spacing the circuit, wires, and high-temperature tag from each other could help prevent of the failure of the high-temperature casing.

5.3 Hot Plate Tests

Hot plate tests allowed for small-scale testing in a realistic environment, similar to the soil box. Heat coming to the sensor from one direction as well as the retained heat of the soil better represents how the sensor will experience heating during a wildfire event, in comparison to oven tests. The hot plate tests were performed at the University of Minnesota and were intended to function as a smaller and easier to conduct soil box test. A steel bowl was placed on a hot plate and 1 inch of compacted soil was placed in the bottom of a steel bowl (Figure 5.15(a)). Three thermocouples were used to track the temperature of the setup; one was placed inside the crucible with the sensing system, another was placed at the bottom of the crucible and a third was fixed to the top of the crucible. A visual temperature indicator was placed on the lid of the crucible, as shown in Figure 5.15 (b). These visual indicators will turn black once the indicator reaches 199°C. The crucible was set inside the bowl on top of the soil and two lifts of soil were added on top, compacting each lift as they occur. The process is shown in Figure 5.15.

Temperatures were recorded every 0.5 seconds until either the threshold temperature was held for 30 minutes or the sensor triggers, whichever happened last. The sensor was read periodically to track at what temperatures and time the sensor triggered. After both the threshold was reached and the Molex tag was unreadable, the hot plate was turned off and was left to cool. Once the system was cooled, the sensor was read again, and the soil was removed to evaluate the sensor system. These tests are only performed using M2, as the system had been the most consistent and dependable of the two designs. Soil moisture was measured for each test with the soil being predominantly silty clay (

Table 5-1). The soil moisture was captured to determine how moisture affected the heating of the system and to compare the heating of the hot plate to the heating of the soil box.

Table 5-1: Soil Moisture Content

Test	Moisture Content (%)
M2hpP1	29.84
M2hpP2	24.5
M2hpH1	21.58
M2hpH2	31.12
M2hpH3	29.07

(a) 1” Compacted soil (b) Sensor Placement (c) Fully compacted system

Figure 5.15: Hot Plate Test Set-up: (a) 1” Compacted Soil, (b) Sensor Placement, (c) Fully Compacted System

Five tests were conducted using the hot plate, two with PVC (M2hpP1 and M2hpP2) and three with HDPE (M2hpH1, M2hpH2, and M2hpH3). Two thermocouples were used for

M1hpP1, one inside and the other at the bottom of the crucible. All other hot plate tests used the three thermocouples. The thermocouple at the bottom of the crucible was used to track the trigger temperature, 194°C and 250°C, respectively. The Molex tag and conductive plate were changed out between tests to ensure that the repeated heating of the system wouldn't negatively impact the test results. For both PVC tests, the trigger material and conductive plate were epoxied together, to ensure the two moved together. The setup for each PVC test is shown below in Figure 5.16. The setup for the HDPE hot plate tests in shown in Figure 5.17.

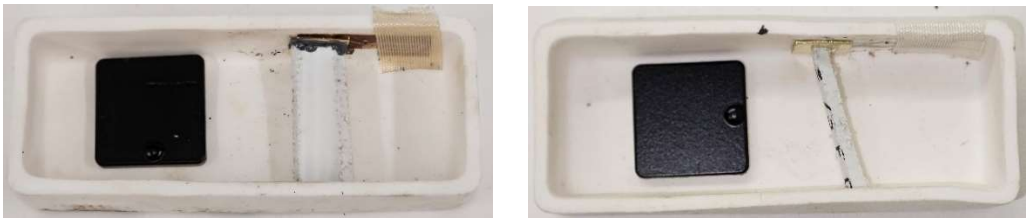

(a) M2hpP1 (b) M2hpP2

Figure 5.16: Hot Plate Test Set-ups: (a) M2hpP1, (b) M2hpP2

(a) M2hpH1 (b) M2hpH2

(c) M2hpH3

Figure 5.17: HDPE Hot Plate Test Set-up: (a) M2hpH1, (b) M2hpH2, (c) M2hpH3

During testing for M2hpP2, the thermocouple inside and on top of the crucible occasionally read values significantly different from the thermocouple on the bottom of the crucible. The top thermocouple showed these erroneous results more often than the thermocouple on the inside of the crucible. To account for this, the bottom thermocouple was used to monitor the heat in the system. Similar to M2hpP2, a few of the thermocouples for the HDPE tests were reading values that deviated from the other thermocouples. In particular, the thermocouple on top of the crucible for M2hpH1 and M2hpH3 had the most variation. These errors happened at regular intervals but would eventually go back to values that more accurately reflected what the other thermocouples were reading. Due to this, the threshold for the HDPE may only have been reached at the bottom of the crucible with limited heat transfer through the height of the soil.

After the PVC systems cooled, the trigger was effective and the M1hpP1 Molex tag did not read, while the M2hpP2 system did not trigger; All the high-temperature tags were still working. The physical results from PVC-based sensor system tests are shown in Figure 5.18. The trigger material for each test did melt as designed, however, as shown in Figure 5.18 (b), the conductive plate was still connected to the Molex tag instead of the trigger material.

(a) M1hpP1 result (b) M1hpP2 result

Figure 5.18: Hot Plate Test Results: (a) M1hpP1, (b) M1hpP

For the HDPE-based sensor tests, all three of the Molex tags were not reading by the time the test concluded. However, after cooling the Molex tag read for both M2hpH1 and M2hpH3. As shown in Figure 5.19, the conductive plate was still attached to the Molex tag in M2hpH1 and M2hpH3, which contributes to the Molex tag still reading.

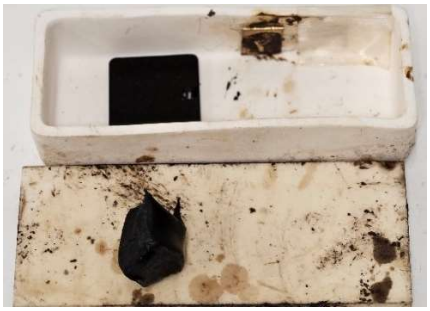

(a) M2hpH1 result

(b) M2hpH2 result

(c) M2hpH3 result

Figure 5.19: HDPE Hot Plate Test Results: (a) M2hpH1, (b) M2hpH2, (c) M2hpH3

Ensuring that the connection between the trigger material and conductive plate is fully formed before heating may help ensure the conductive plate moved with the trigger material in future tests. Additionally, using the thermocouple on the bottom of the crucible to monitor the temperature of the system does not accurately represent the temperature that the crucible is

exposed to around the system. For M1hpP1 and M1hpP2 tests, the visual indicators (Figure 5.20) did not trigger, as was expected, because the temperatures for these tests should be below 199°C, while the HDPE tests should trigger the visual indicator. From Figure 5.20 (c), the visual indicator did not trigger, indicating that the M2hpH1 sensor only experienced the threshold temperature from the bottom of the crucible to somewhere below the location of the indicator tag. Additionally, the heat being released from the system could affect the signal being sent and received from the RFID antenna, which could lead to false negative results from the sensors during testing. This could be why all the Molex tags weren't reading at the end of the HDPE hot plate tests, but the Molex tag for M2hpH1 and M2hpH3 were still readable once the system cooled.

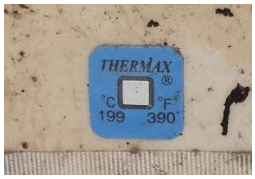

(a) M2hpP1

(b) M2hpP2

(c) M2hpH1

(b) M2hpH2

(e) M1hpH3

Figure 5.20: Visual Indicator Results: (a) M1hpP1, (b) M1hpP2, (c) M1hpH1, (d) M1hpH2, (e) M1hpH3

The long-term reliability of the sensors has not been monitored but should be considered going forward. Currently, brass is being used for the conductive plate, however, it will be important to test the material for long-term use, as the humidity may cause issues. From the oven

tests, design M2 seems more reliable than design M1, however, due to the location of the cut in the antenna tag, the read range of the Molex in M2 is much shorter than the read range of M1. This limited read range could cause issues if the sensors need to be placed deeper in the soil.

In summary, all three tests performed on the sensor systems have merit. The soil box and hot plate tests allowed the sensors to be exposed to an environment closer to an actual wildfire, while the oven tests allow testing the system in a controlled environment. While in the oven, the heat is known throughout the system and can be controlled easily, while the soil box and hot plate tests will expose the sensors to residual heat, which is something the oven won't replicate as well.

Chapter 6. Conclusion

Wildfires can have a devastating impact on communities, and of particular interest is the potential for contamination the water supply in WUI regions. These contaminations occur in polymer-based pipelines, specifically PVC and HDPE systems. Developing a sensor system that can easily detect if a pipe or section of pipes needs to be tested for VOCs and possibly replaced will aid recovery of affected communities. A passive RFID sensing system has been developed using off-the-shelf components as a cost-effective solution that should last communities for years to come. A passive RFID tag is integrated with a temperature-triggered circuit whose readability is dependent on the threshold being met. The other tag is a high-temperature ceramic encased RFID tag, which indicated the pipe being read and limits the likelihood of false positives. A trigger material is used as a temperature threshold sensor, where the material is chosen based on the pipeline being monitored: for a PVC pipeline, PVC will be used as the trigger material, and HDPE will be used as its trigger. After a wildfire event, communities which have implemented this system will be able to place a reader over a general cluster of pipelines. If only the high-temperature tag is being read, or only the high-temperature ID is showing for a particular pipe, future inspection of the pipe should be considered.

Two models were designed and tested using both benchtop and more realistic testing environments. Model 2, which has a simpler trigger circuit, is the most efficient, consistent, and cost-effective of the two. Outside of the two designs. Future work on Model 2, should consider the impact of the design on the buried sensor read range and how long-term environmental exposure might inform material selections.

Chapter 7. References

[1] Abdelnour, A., A. Lazaro, R. Villarino, D. Kaddour, S. Tedjini, and D. Girbau. 2018. "Passive Harmonic Rfid System for Buried Assets Localization." *Sensors (Switzerland)* 18 (11). MDPI AG. https://doi.org/10.3390/s18113635.

[2] Amendola, S., R. Lodato, S. Manzari, C. Occhiuzzi, and G. Marrocco. 2014. "RFID Technology for IoT-Based Personal Healthcare in Smart Spaces." *IEEE Internet of Things Journal* 1 (2). 144–52. doi:10.1109/JIOT.2014.2313981.

[3] Aroca R. V., A. C. Hernandes, D. V. Magalhães, M. Becker, C. M. P. Vaz & A. G. Calbo. 2018. "Calibration of Passive UHF RFID Tags Using Neural Networks to Measure Soil Moisture," *Journal of Sensors*, 2018 (2018), 1-12. https://doi.org/10.1155/2018/3436503

[4] Babar, A. A., V. A. Bhagavati, L. Ukkonen, A. Z. Elsherbeni, P. Kallio, L. Sydänheimo. 2012 "Performance of High-Permittivity Ceramic-Polymer Composite as a Substrate for UHF RFID Tag Antennas", *International Journal of Antennas and Propagation*, (2012), 1-8. https://doi.org/10.1155/2012/905409

[5] Babar, A. Ali, T. Björninen, V. A. Bhagavati, L. Sydänheimo, P. Kallio, and L. Ukkonen. 2012. "Small and Flexible Metal Mountable Passive UHF RFID Tag on High-Dielectric Polymer-Ceramic Composite Substrate." *IEEE Antennas and Wireless Propagation Letters* 11, 1319–22. https://doi.org/10.1109/LAWP.2012.2227291.

[6] Badar, M., Y.D. Sum, F. Lu, P. Lu, M. Buric, P. Ohodnicki, 2021. "Low-cost optical fiber based temperature sensor for real-time health monitoring of power transformers." Proc. SPIE 11939, https://doi.org/10.1117.12.2587114

[7] Bauer-Reich, C., K.C. Tan, F. Haring, N. Schneck, A. Wick, L. Berge, J. Hoey, R. Sailer, C. Ulven. 2014. "An investigation of the viability of UHF RFID for subsurface soil sensors," *IEEE International Conference on Electro/Information Technology*, 577-580. https://doi.org/ 10.1109/EIT.2014.6871828.

[8] Bhattacharyya, R., C. Floerkemeier, and S. Sarma. 2010. "RFID Tag Antenna Based Temperature Sensing." In RFID 2010: *International IEEE Conference on RFID*: 8–15. https://doi.org/10.1109/RFID.2010.5467239.

[9] Caizzone, S., C. Occhiuzzi, and G. Marrocco. 2011. "Multi-Chip RFID Antenna Integrating Shape-Memory Alloys for Detection of Thermal Thresholds." *IEEE Transactions on Antennas and Propagation* 59 (7): 2488–94. https://doi.org/10.1109/TAP.2011.2152341.

[10] Cal Fire. 2019a. "Tubbs Fire." *California Department of Forestry and Fire Protection.* Accessed May 2023.

[11] Cal Fire. 2019b "Camp Fire." May 2023, *California Department of Forestry and Fire Protection*. Accessed May 2023.

[12] Crenshaw, B. R., J. Kunzelman, C. E. Sing, C. Ander, and C. Weder. 2007. "Threshold Temperature Sensors with Tunable Properties." *Macromolecular Chemistry and Physics* 208 (6): 572–80. https://doi.org10.1002/macp.200600622.

[13] Dowling, J., M. Tentzeris, and N. Beckett. 2009. “RFID-Enabled Temperature Sensing Devices: A Major Step Forward for Energy Efficiency in Home and Industrial Applications*?” In IEEE MTT-S International Microwave Workshop Series on Wireless Sensing, Local Positioning and RFID, Proceedings, IMWS 2009 - Croatia*. https://doi.org/10.1109/IMWS2.2009.5307884.

[14] Amin, E. M., J. K. Saha, and N. C. Karmakar. 2014. “Smart Sensing Materials for Low-Cost Chipless RFID Sensor.” *IEEE Sensors Journal* 14 (7): 2198–2207. https://doi.org10.1109/JSEN.2014.2318056.

[15] Franchina V., A. Ria, A. Michel, P. Bruschi, P. Nepa and A. Salvatore, "A Compact UHF RFID Ceramic Tag for High-Temperature Applications," *2019 IEEE International Conference on RFID Technology and Applications (RFID-TA)*, 2019: 480-483, https://doi.org/10.1109/RFID-TA.2019.8892217.

[16] Hamrita T. K., and E. C. Hoffacker. 2005 “Development of a “smart” wireless soil monitoring sensor prototype using RFID technology” *Applied Engineering in Agriculture* 21 (1): 1939-143

[17] Hamideh, S., P. Sen, E. Fischer. 2022. “Wildfire impacts on education and healthcare: Paradise, California, after the Camp fire.” *Natural Hazards.* 111: 353-387, https://doi.org/10.1007/s11069-021-05057-1

[18] Hauser, R., R. Fachberger, G. Bruckner, R. Reicher, and W. Smetana. 2005. “Ceramic Patch Antenna for High-Temperature Applications.” In *28th International Spring Seminar on Electronics Technology: Meeting the Challenges of Electronics Technology Progress, 2005*, 2005:159–64. https://doi.org/10.1109/ISSE.2005.1491022.

[19] Huang H., J. Shi, F. Wang, D. Zhang, & D. Zhang. 2020. “Theoretical and experimental studies on the signal propagation in soil for wireless underground sensor networks,” *Sensors (Switzerland)*, 20 (9). https://doi.org/10.3390/s20092580

[20] Kramer, H.A., V. Butic, M. H. Mockrin, C. Ramirez-Rayes, P. M. Alexandre, V. C. Radeloff. 2021. “Post-wildfire rebuilding and new development in California indicated minimal adaption to fire risk.” Land Use Policy 107; https://doi.org/10.1016/j.landusepol.2021.105502

[21] Khan, Z., X. Chen, H. He, A. Mehmood, and J. Virkki. 2021. “A Bending Passive RFID Tag as a Sensor for High-Temperature Exposure.” *International Journal of Antennas and Propagation*. Hindawi Limited. https://doi.org/10.1155/2021/5541197.ultrahigh-frequency

[22] Isaacson, K. P., C. R. Proctor, Q. E. Wang, E. Y. Edwards, Y. Noh, A. D. Shah, and A. J. Whelton. 2020. “Drinking water contamination from the thermal degradation of plastics: implications for wildfire and structure fire response.” *Environment Science: Water Research & Technology*, 7: 274-284, https://doi.org/10.1039/D0EW00836B

[23] Inaudi, D., and B. Glisic. 2010. “Long-Range Pipeline Monitoring by Distributed Fiber Optic Sensing.” *Journal of Pressure Vessel Technology, Transactions of the ASME* 132 (1): 0117011–19. https://doi.org/10.1115/1.3062942

[24] Lin, T. H., Y. Wu, K. Soga, B. P. Wham, C. Pariya-Ekkasut, B. Berger, & T.D. O’Rourke, T. (2019). “Buried Wireless Sensor Network for Monitoring Pipeline Joint Leakage

Caused by Large Ground Movements," *Journal of Pipeline Systems Engineering and Practice*, *10*(4). https://doi.org/10.1061/(asce)ps.1949-1204.0000392

[25] Liu, Y., F. Deng, Y. He, B. Li, Z. Liang, and S. Zhou. 2017. "Novel Concrete Temperature Monitoring Method Based on an Embedded Passive RFID Sensor Tag." *Sensors (Switzerland)* 17 (7). MDPI AG. https://doi.org/10.3390/s17071463.

[26] Fiddes, Lindsey K., and Ning Yan. 2013. "RFID Tags for Wireless Electrochemical Detection of Volatile Chemicals." *Sensors and Actuators, B: Chemical* 186. Elsevier B.V.: 817–23. https://doi.org/10.1016/j.snb.2013.05.008.

[27] Mishra P. K., R. F. Stewart, M. Bolic and M. C. E. Yagoub. 2014. "RFID in Underground-Mining Service Applications," in *IEEE Pervasive Computing*, 13, (1): 72-79, Jan.-Mar. 2014, https://doi.org/10.1109/MPRV.2014.14.

[28] "Model C2525-H3 Ceramic RFID Tag. Specifications & Data Sheet," Accessed March 30, 2023, UHF Mid Range Reader (rfidinc.com)

[29] Nikles, Marc. 2009. "Long-Distance Fiber Optic Sensing Solutions for Pipeline Leakage, Intrusion, and Ground Movement Detection." In *Fiber Optic Sensors and Applications VI*, 7316:731602. SPIE. https://doi.org/10.1117/12.818021.

[30] Nikles, Marc, Bernhard H. Vogel, Fabien Briffod, Stephan Grosswig, Florian Sauser, Steffen Luebbecke, Andre Bals, and Thomas Pfeiffer. 2004. "Leakage Detection Using Fiber Optics Distributed Temperature Monitoring." In *Smart Structures and Materials 2004: Smart Sensor Technology and Measurement Systems*, 5384:18. SPIE. https://doi.org10.1117/12.540270.

[31] Occhiuzzi, C., S. Caizzone, and G. Marrocco. 2013. "Passive UHF RFID Antennas for Sensing Applications: Principles, Methods, and Classifications." *IEEE Antennas and Propagation Magazine* 55 (6). IEEE Computer Society: 14–34. https://doi.org/10.1109/MAP.2013.6781700

[32] Proctor, C., J. Lee, D. Yu, A. D. Shah, A. J. Whelton. 2020. "Wildfire Caused Widespread Drinking Water Distribution Network Contamination." *AWWA Water Science,* 2 (4): e1183, https://10/1002/AWS2.1183

[33] Reinisch, H., M. Wiessflecker, S. Gruber, H. Unterassinger, G, Hofer, M. Klamminger, W. Pribyl, G. Holweg. 2011. "A Multifrequency Passive Sensing Tag with On-Chip Temperature Sensor and Off-Chip Sensor Interface Using EPC HF and UHF RFID Technology," in *IEEE Journal of Solid-State Circuits*, 46 (12): 3075-3088, https.//doi.org/10.1109/JSSC.2011.2167548.

[34] Ria, A., A. Michel, R. K. Singh, V. Franchina, P. Bruschi and P. Nepa, 2020. "Performance Analysis of a Compact UHF RFID Ceramic Tag in High-Temperature Environments," *IEEE Journal of Radio Frequency Identification*, 4 (4): 461-467, https://doi.org/10.1109/JRFID.2020.2998008.

[35] Richter, E. G. "Simulation of Heat Transfer Through Soil for the Investigation of Wildfire Impacts on Buried Utilities." M.S. thesis, Oregon State University.

[36] Richter, E. G., E. C. Fischer, A. Metz, and B. P. Wham. 2022. “Simulation of Heat Transfer Through Soul for the Investigation of Wildfire Impacts on Buried Pipelines.” *Fire Technology,* https://doi.org/10.1007/s10694-022-01232-3

[37] Schulze, S. S., and E. C. Fischer. 2021. “Prediction of Water Distribution System Contamination Based on Wildfire Burn Severity in Wildland Urban Interface Communities.” *ACS ES&T Water* 1 (2): 291-299, https://doi.org/ acsestwater.0c00073

[38] Schulze, S. S., E. C. Fischer, S. Hamideh, and H. Mahmoud. 2020. “Wildfire impacts on schools and hospitals following the 2018 California Camp Fire.” *Natural Hazards* 104: 901-925. https://doi.org/10.1007/s11069-020-04197-0

[39] Silva, B., R. M. Fisher, A. Kumar, and G. P. Hancke. 2015. “Experimental Link Quality Characterization of Wireless Sensor Networks for Underground Monitoring.” *IEEE Transactions on Industrial Informatics* 11 (5). IEEE Computer Society: 1099–1110. https://doi.org/10.1109/TII.2015.2471263.

[40] Sing, C. E., J. Kunzelman, and C. Weder. 2009. “Time-Temperature Indicators for High Temperature Applications.” *Journal of Materials Chemistry* 19 (1): 104–10. https://doi.org/10.1039/b813644k.

[41] Ukil, A., H. Braendle, and P. Krippner. 2012. “Distributed Temperature Sensing: Review of Technology and Applications.” *IEEE Sensors Journal*. https://doi.org/10.1109/JSEN.2011.2162060.

[42] Virtanen, J., L. Ukkonen, T. Björninen, L. Sydañheimo, and A. Z. Elsherbeni. 2011. “Temperature Sensor Tag for Passive UHF RFID Systems.” In *SAS 2011 - IEEE Sensors Applications Symposium, Proceedings*, 312–17. https://doi.org/10.1109/SAS.2011.5739788.

[43] “VPC 1/2 in. X 24 in. PVC SCH. 40 pipe 22015.” (n.d.). *The Home Depot*. Accessed Apr. 4, 2023. https://www.homedepot.com/p/VPC-1-2-in-x-24-in-PVC-Sch-40-Pipe-22015/202300504

[44] Vyas, R., and B. Tye. 2019. “A Sequential RFID System for Robust Communication with Underground Carbon Steel Pipes in Oil and Gas Applications.” *Electronics (Switzerland)* 8 (12). MDPI AG. https://doi.org/10.3390/electronics8121374.

[45] Wang, X., J. Zhang, Z. Yu, S. Mao, S. C. G. Periaswamy and J. Patton. 2019. "On Remote Temperature Sensing Using Commercial UHF RFID Tags," *IEEE Internet of Things Journal*, 6 (6): 10715-10727, https://doi.org/10.1109/JIOT.2019.2941023.

[46] Whelton, A. J., C. Seidel, B. P. Wham, E. C. Fischer, K. Isaacson, C. Jankowski, N. MacArther, E. Mckenna, and C. Ley. 2023. “The Marshall Fire: Scientific and policy needs for water system disaster response.” *AWWA Water Science* 5 (1): e1318. https://doi.org/10.1002/aws2/1318

[47] Zhang, J., G.Y. Tian, A. M. J. Marindra, A. I. Sunny, and A. B. Zhao. 2017. “A Review of Passive RFID Tag Antenna-Based Sensors and Systems for Structural Health Monitoring Applications. *Sensors (Switzerland)*. https://doi.org/10.3390/s17020265

[48] 2023. “Molex, part 0133580821 Specifications.” *Molex.* Accessed March 30, 2023, 0133580821_ANTENNAS.pdf (molex.com)